The effects of diachronous surface uplift of the European Alps on regional climate and the oxygen isotopic composition of precipitation

Daniel Boateng[1*], Sebastian G. Mutz[1], Armelle Ballian[2,3], Maud J. M. Meijers[4], Katharina Methner[2,5], Svetlana Botsyun[6], Andreas Mulch[2,3], Todd A. Ehlers[1]

[1]Department of Geosciences, University of Tübingen, Tübingen, Germany
[2]Senckenberg Biodiversity and Climate Research Centre, Frankfurt am Main, Germany
[3]Goethe University Frankfurt Institute of Geoscience, Frankfurt am Main, Germany
[4]Institute of Earth Sciences, NAWI Graz Geocenter, University of Graz, Austria
[5]Department of Geophysics and Geology, University of Leipzig, Leipzig, Germany
[6]Institute of Meteorology, Freie Universität Berlin, Berlin, Germany

Correspondence to: daniel.boateng@uni-tuebingen.de

Summary

Additional results from the topography experiments are presented here. The reader is advised to check Table 1 or section 2.2 of the main text to understand the exact meanings of the experiment labels (as also shown in Fig. S1). Since only the seasonal, long-term mean differences (i.e., ID - CTL) are shown and discussed in the main text, the absolute values for long-term seasonal means are shown in supplemental figures S2, S3, and S4. Moreover, the annual long-term mean differences are shown in figures S5, S6, and S7, and the annual-scale isotopic lapse rates in figures S9 and S10. Spatial profiles that compare the diachronous surface uplift to the bulk surface uplift scenarios show distinct patterns of isotopic signals across the Alps (Fig. S8). Moreover, our results suggest less different patterns of back trajectories in response to differentiated surface uplift to the west and north flank of the Alps (i.e., Lyon and Munich, respectively) (Fig. S11 and S12).

In the investigation of the impacts of surface uplift on summer teleconnection patterns, Empirical Orthogonal Function (EOF) analysis results from ERA5 data (Fig. S13) were used to guide our discussion in the main text. This analysis is focused on the four leading EOFs that represent the dominant teleconnection patterns in Europe. More specifically, the first EOF (explained variance of 27.35%) shows north-south dipole patterns with maximum negative anomalies region across Iceland and Greenland and with maximum positive anomalies across the North Atlantic (near the Azores). The second EOF shows a monopole axis of positive anomalies across the Atlantic towards Europe, with the main center of action over Ireland and the UK (Fig. 13 B). The third EOF shows dipole patterns of positive anomalies over the Atlantic and negative anomalies across northeast Europe extending in the southeast direction (Fig. 13 C). Lastly, the fourth EOF shows three main centers of action with negative anomalies over western Russia and the Atlantic and positive anomalies over Ireland and the UK (Fig. 13 D).
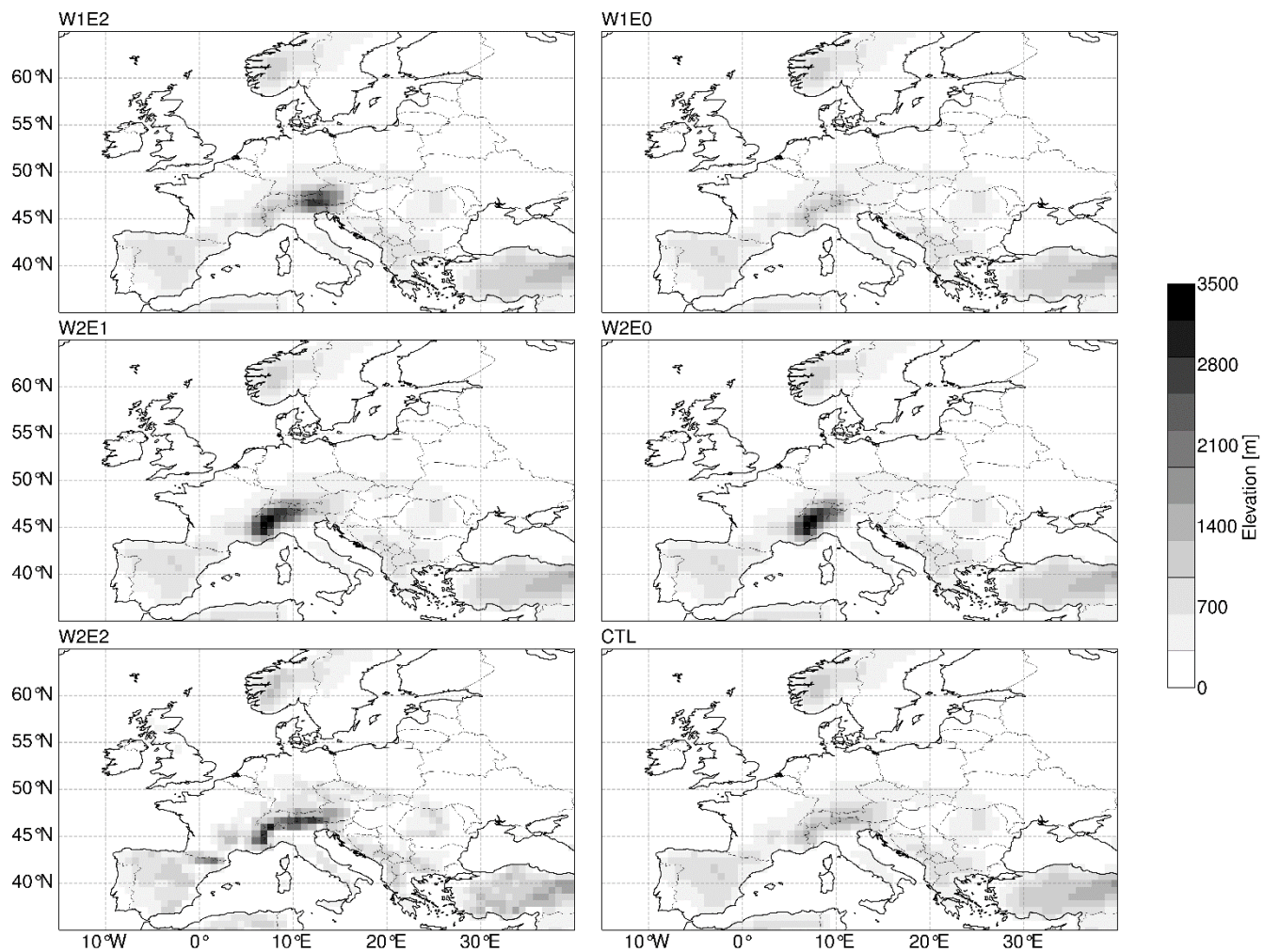
35 **Figure S1: Topographic configurations that were used as the surface boundary conditions for the GCM sensitivity experiments.**
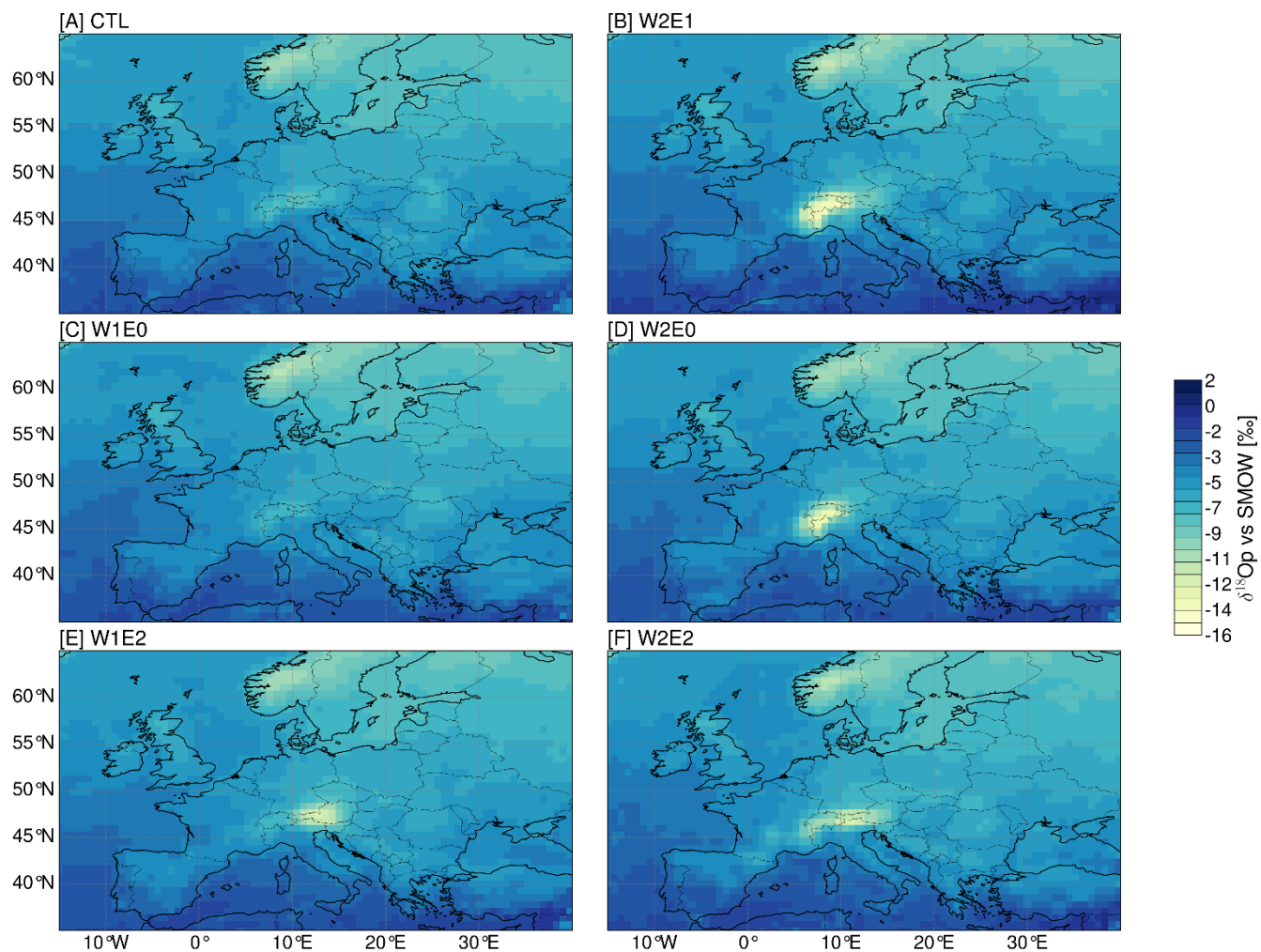
Figure S2: Seasonal (JJA) means of δ¹⁸Oₚ values in response to the different topography scenarios.
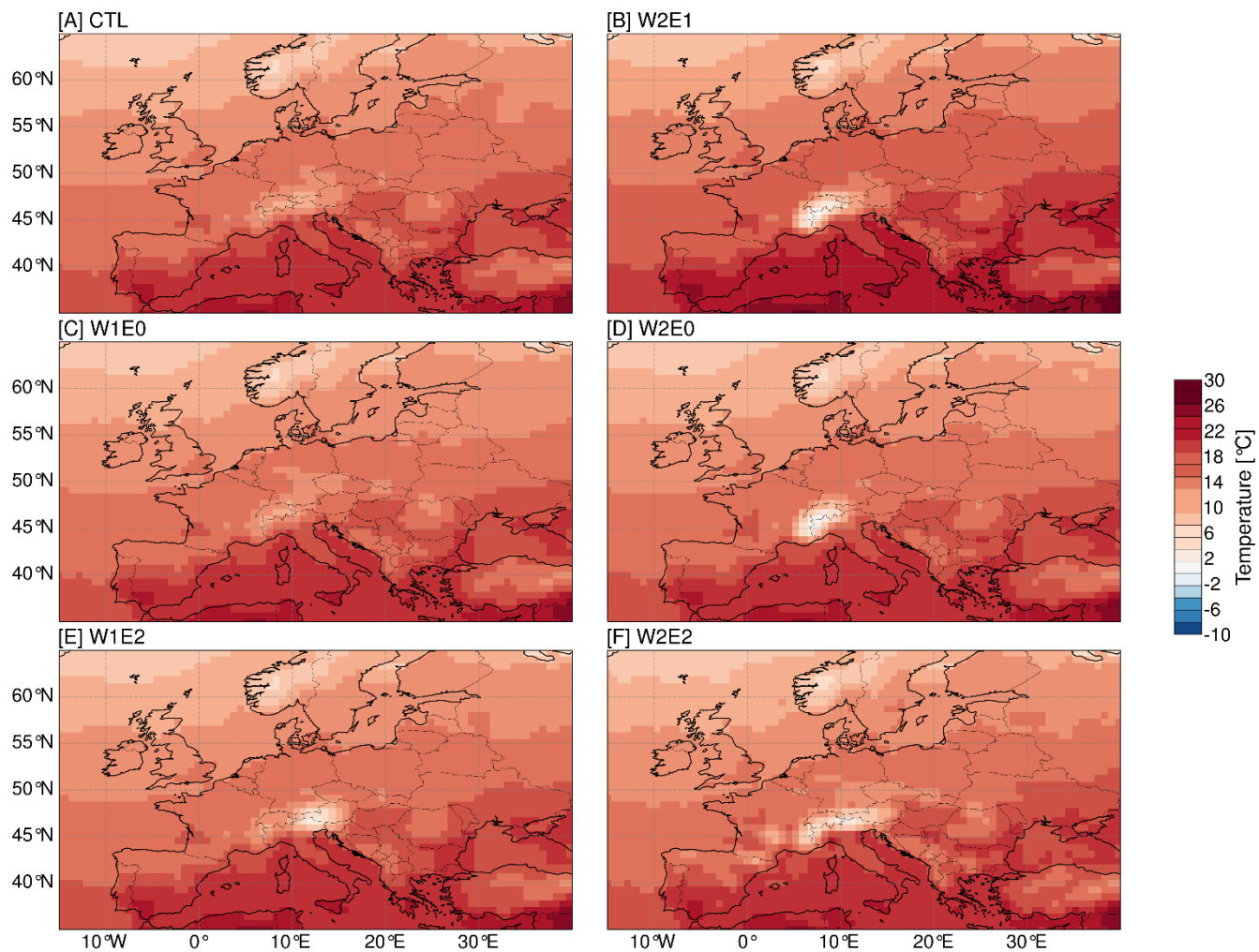
Figure S3: Seasonal (JJA) means of near-surface temperature in response to the different topography scenarios.

40
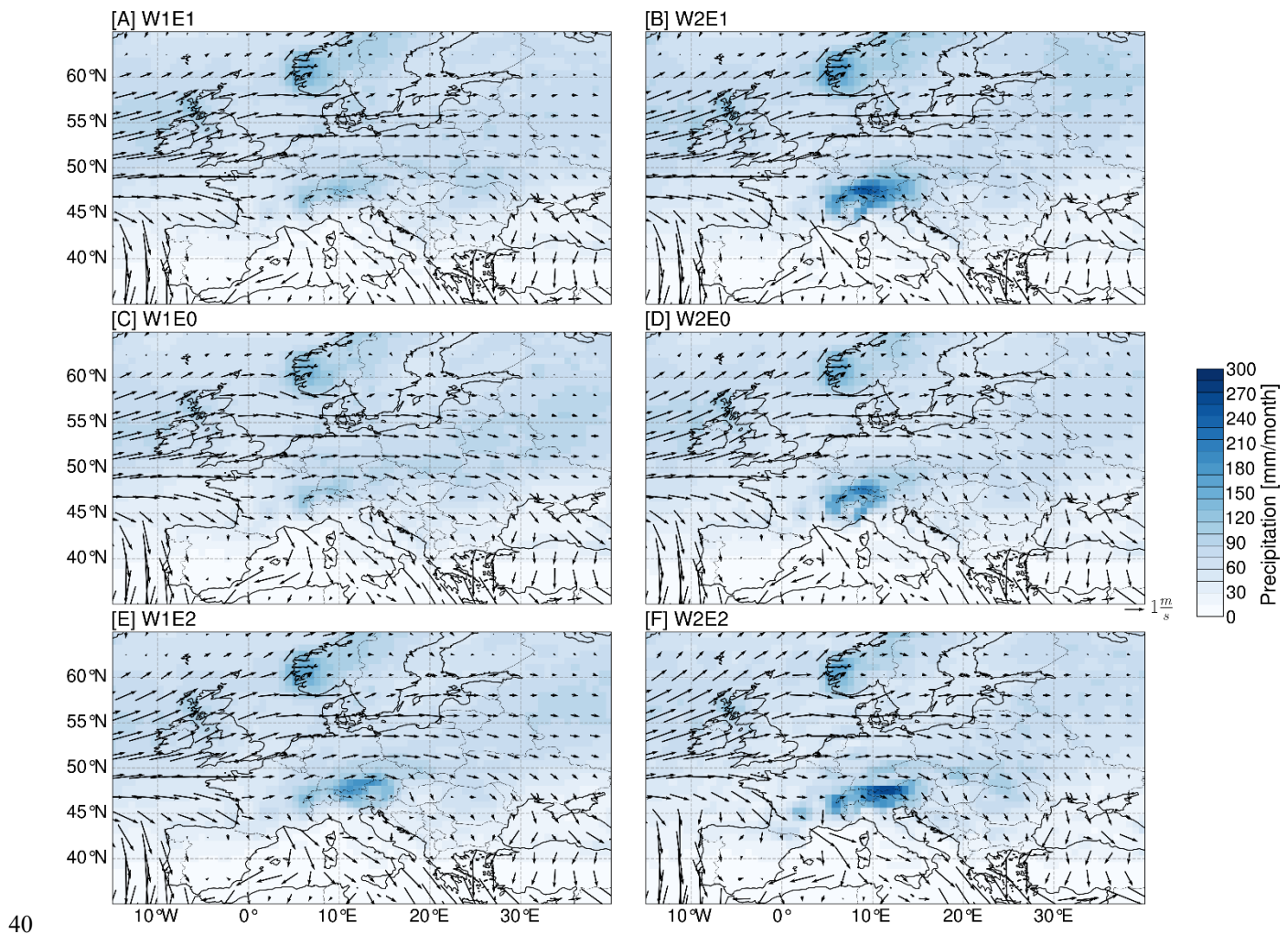
Figure S4: Seasonal (JJA) means of precipitation amount (colored shading) and near-surface wind patterns (arrows) in response to the different topography scenarios.
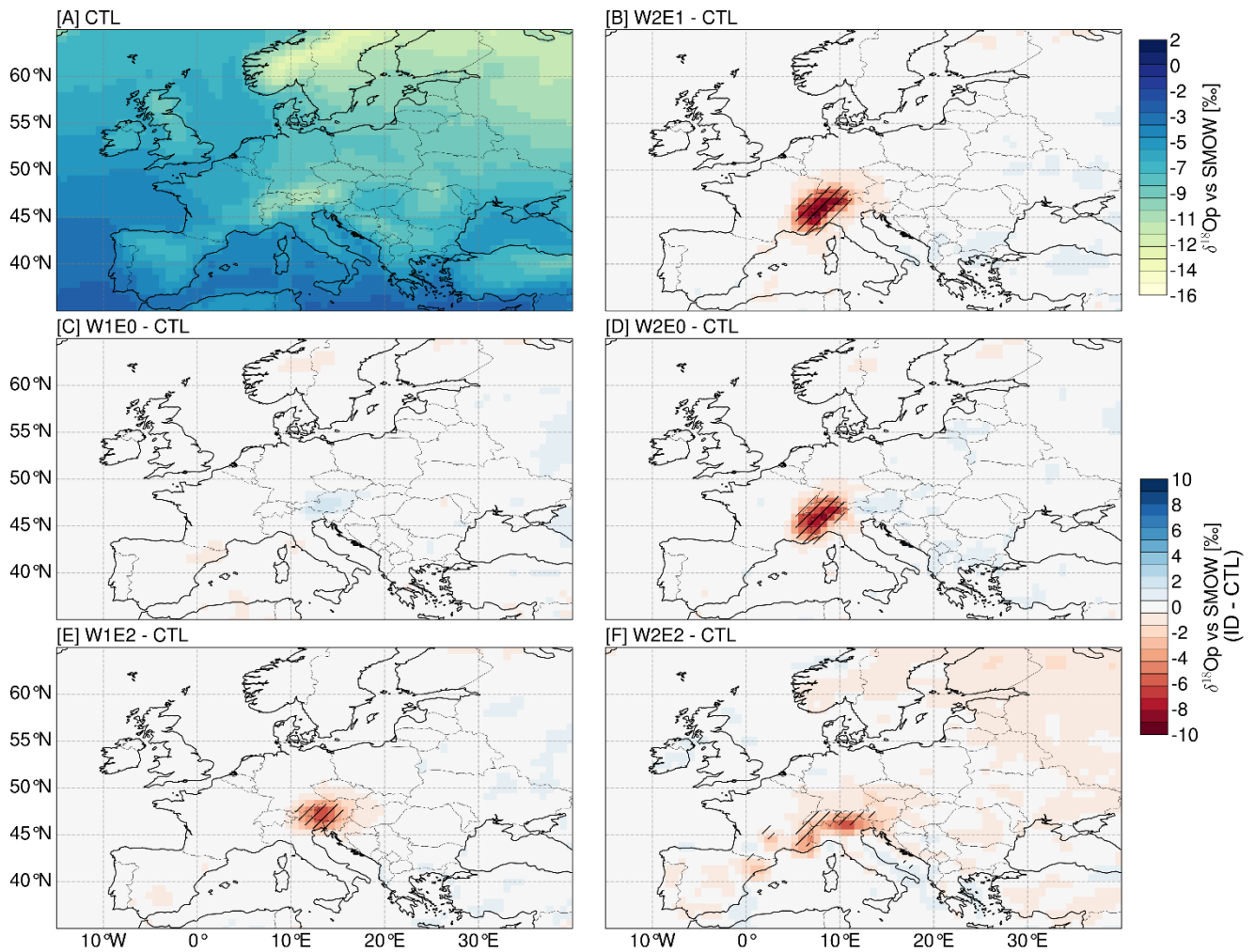
Figure S5: Annual means of δ¹⁸Oₚ values for the CTL experiment (A) and mean differences (i.e., W2E1-CTL (B), W1E0-CTL (C), W2E0-CTL (D), W1E2-CTL (E) and W2E2-CTL (F)) for the topographic scenarios. Red color ranges represent more depleted, and blue color ranges represent a more enriched isotopic composition than in the control experiment. Regions that experience changes that are statistically significant, as indicated by student t-test analysis with a 95% confidence level, are marked with black slash stippling.
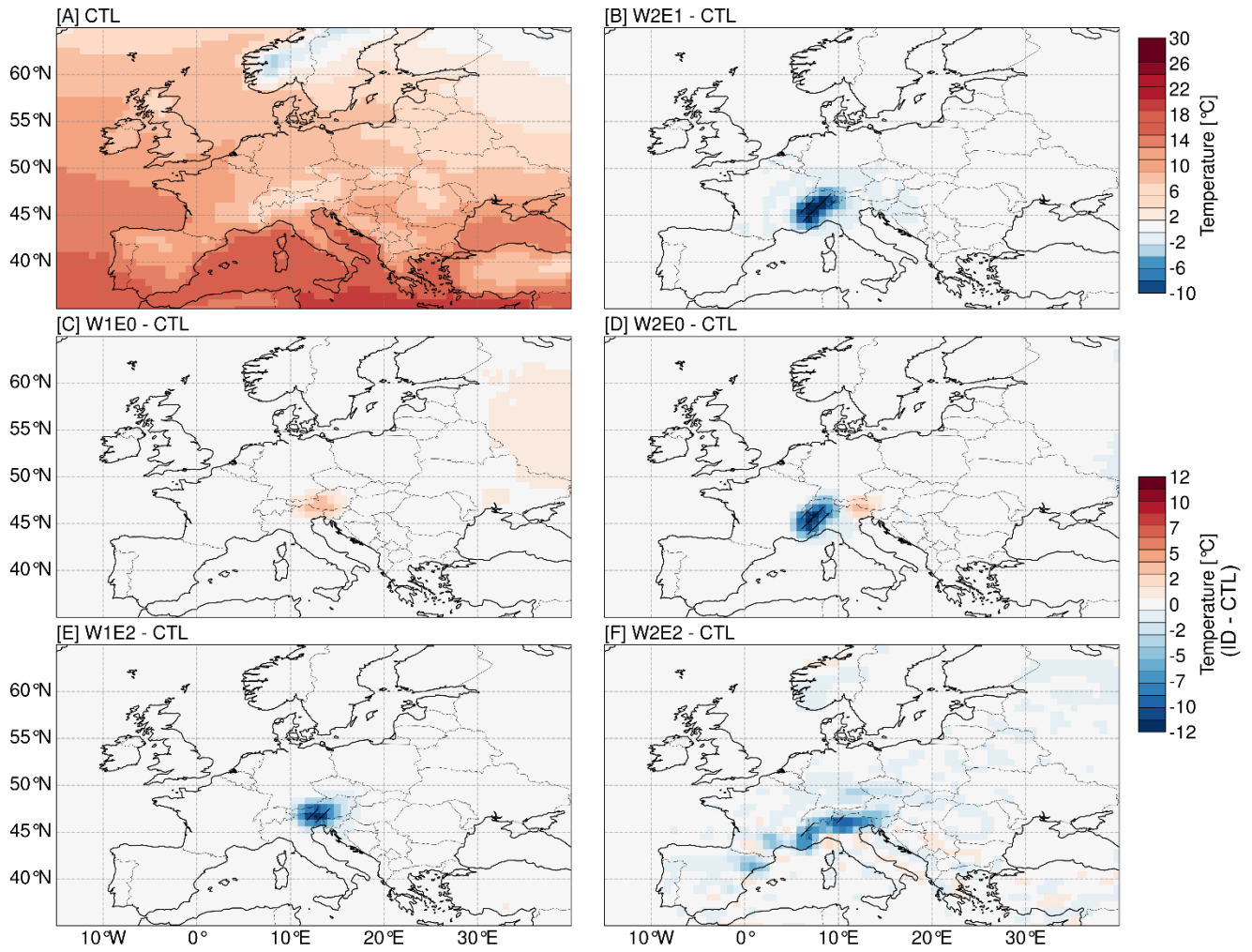
Figure S6: Annual means of near-surface temperature for the CTL experiment (A) and mean differences (i.e., W2E1-CTL (B), W1E0-CTL (C), W2E0-CTL (D), W1E2-CTL (E) and W2E2-CTL (F)) for the topography scenarios. Red color ranges represent warmer, and blue color ranges represent colder temperatures than in the CTL experiment. Regions that experience changes that are statistically significant, as indicated by student t-test analysis with a 95% confidence level, are marked with black slash stippling.

55
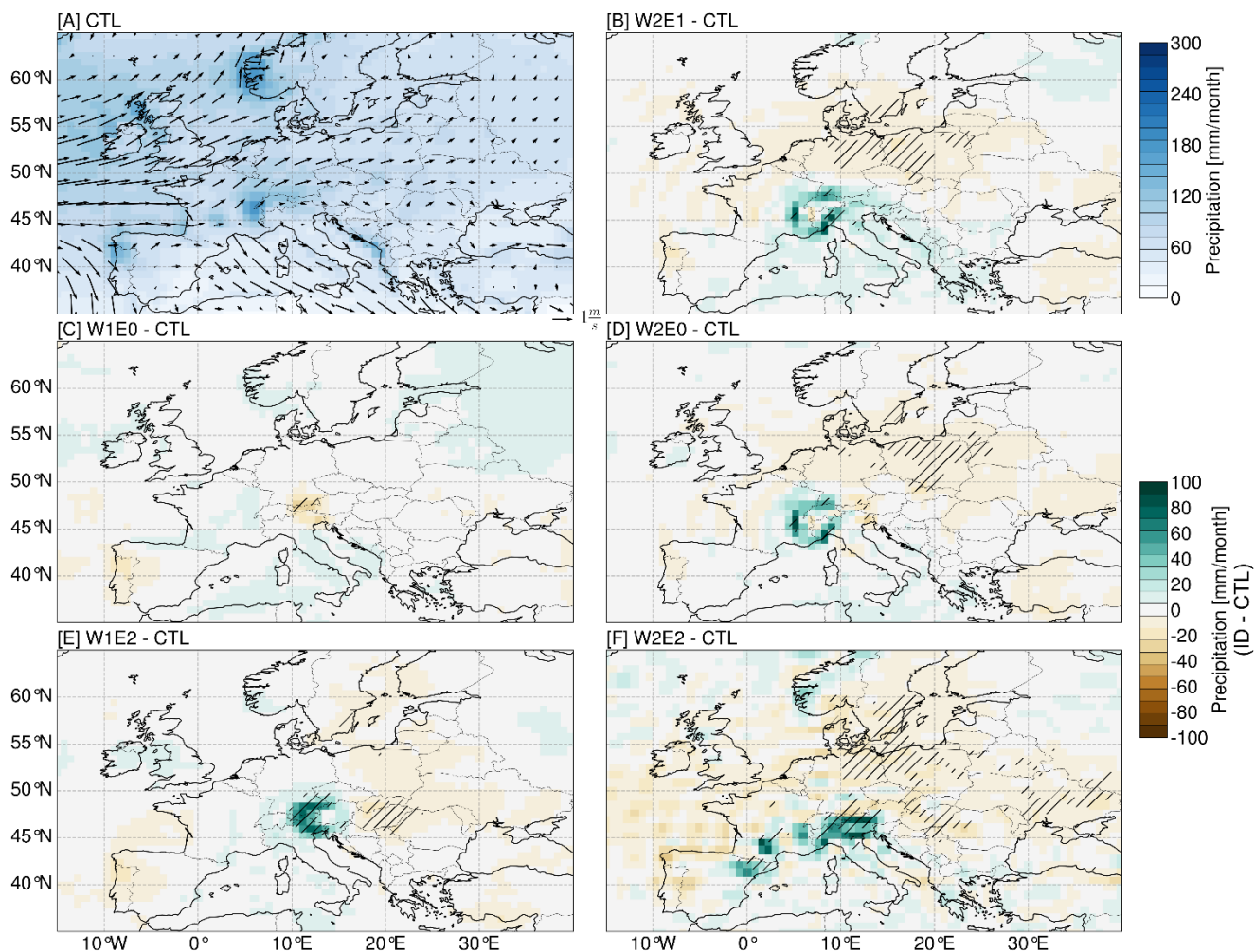
Figure S7: Annual means of precipitation for the CTL experiment (A) and mean differences (i.e., W2E1-CTL (B), W1E0-CTL (C), W2E0-CTL (D), W1E2-CTL (E) and W2E2-CTL (F)) for the topography scenarios. Green color ranges represent wetter, and brown color ranges represent drier conditions than in the CTL experiment. Regions that experience changes that are statistically significant, as indicated by student t-test analysis with a 95% confidence level, are marked with black slash stippling.

60
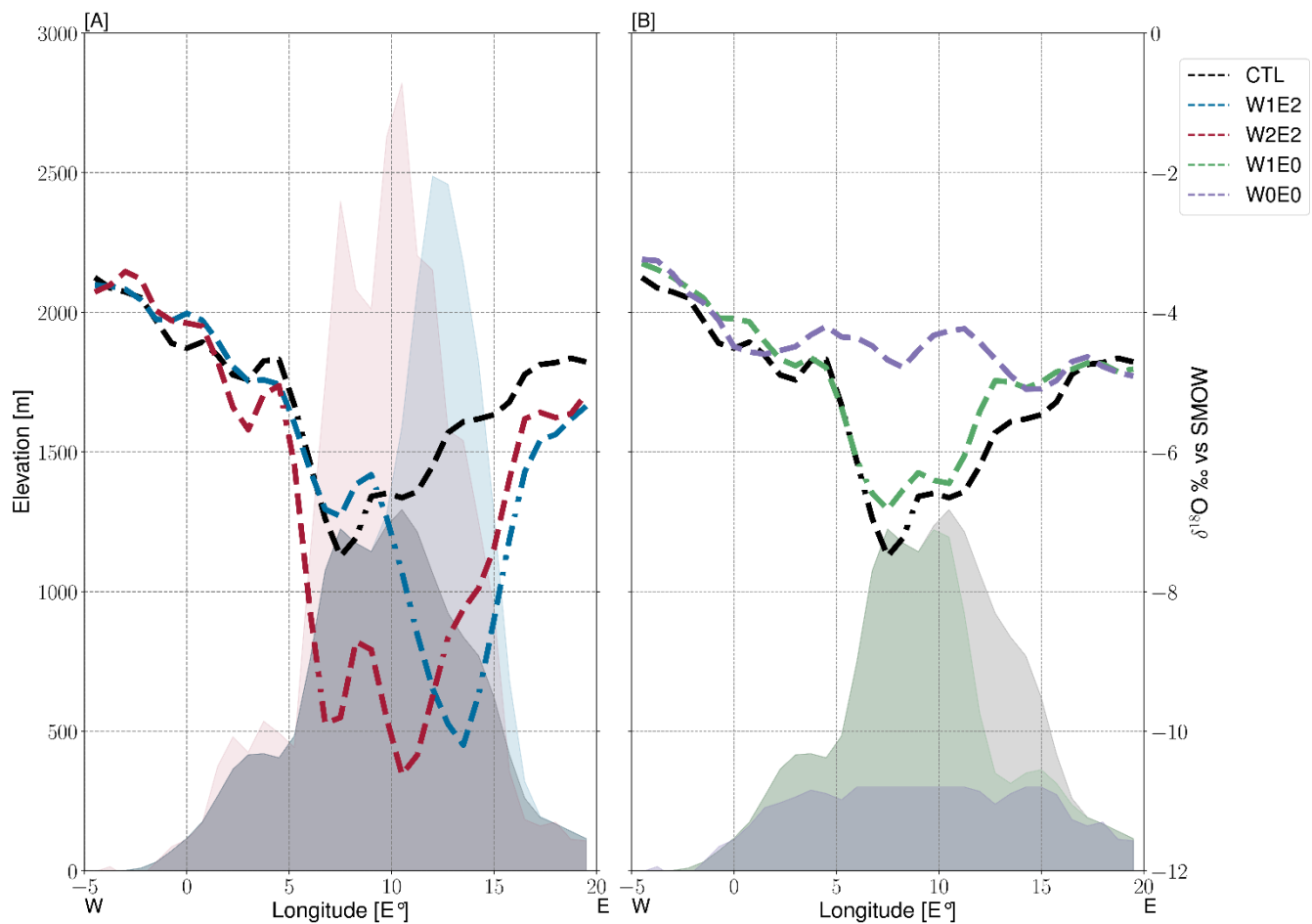
Figure S8: Regional seasonal (JJA) means of spatial δ¹⁸Oₚ values across the Alps in longitudinal (averaged between 46°N and 47°N) (A, C) direction in response to the different topography configurations (CTL (black), W1E0 (green), W1E2 (blue), W0E0 (purple) and W2E2 (red)). The color shadings represent the topographic configuration of both bulk surface uplift or reduction and diachronous surface uplift scenarios.
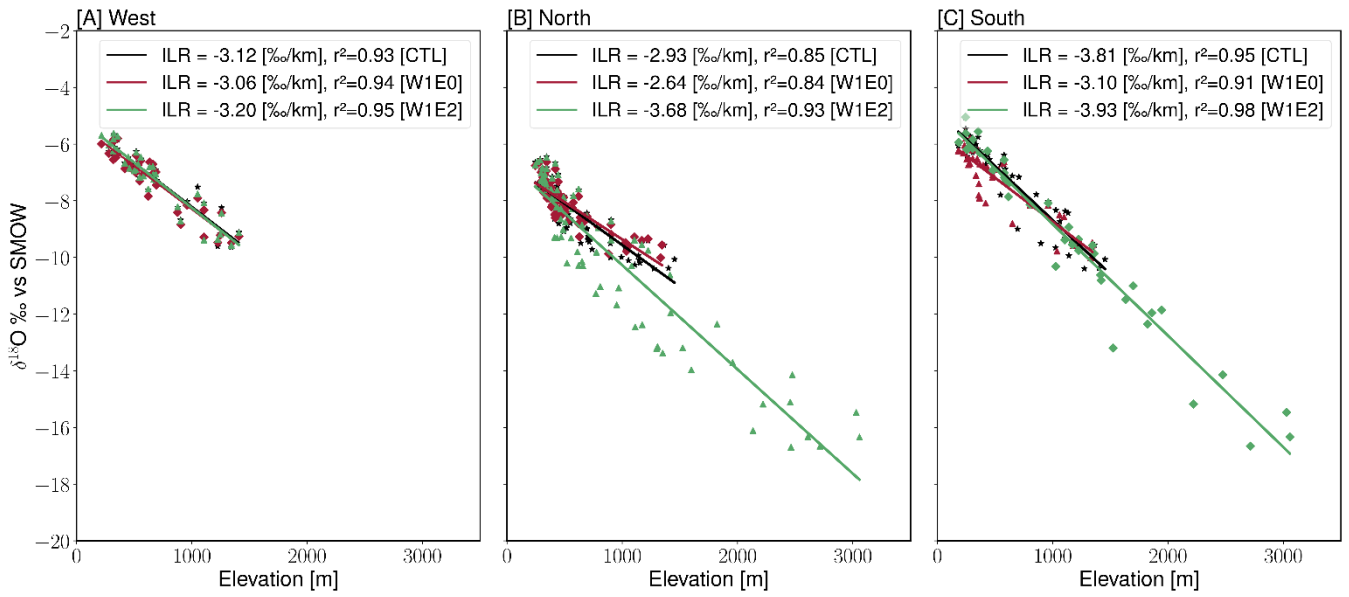
Figure S9: Empirical annual isotopic lapse rates (ILR) estimates for the W1 topography configurations (i.e., W1E0 (red), W1E2 (green)), and CTL (black) for the different transects around the Alps as shown in Fig. 1 A (West: 44 - 47 °N, 1- 8 °E, south: 43 - 47 °N, 8 -15 °E, and north: 47 - 50 °N, 5-16 °E). The ILRs are estimated as the $\delta^{18}O_p$-elevation gradients using linear regression. The r^2 values represent the associated correlation coefficients.
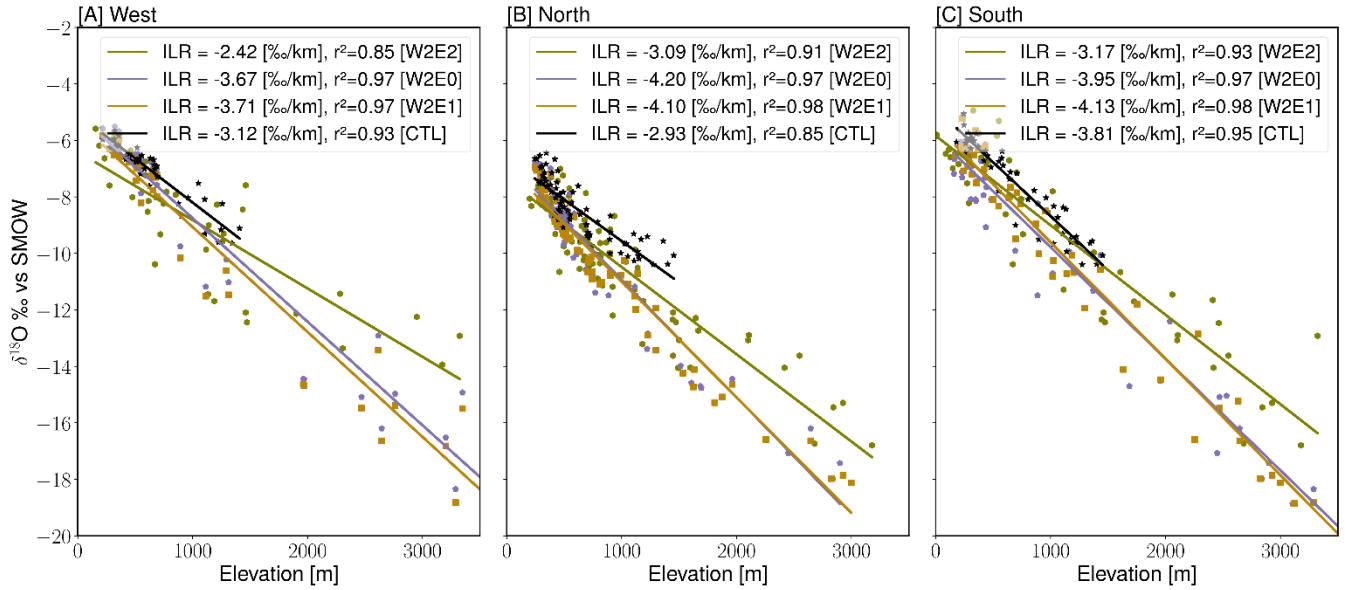
Figure S10: Empirical annual isotopic lapse rates (ILR) estimates for the W2 topography configurations (i.e., W2E0 (purple), W2E1 (gold)), CTL (black), and W2E2 (olive) for the different transects around the Alps as shown in Fig. 1 A (West: 44 - 47 °N, 1- 8 °E, south: 43 - 47 °N, 8 -15 °E, and north: 47 - 50 °N, 5-16 °E). The ILRs are estimated as the $\delta^{18}O_p$-elevation gradients using linear regression. The r^2 values represent the associated correlation coefficients.
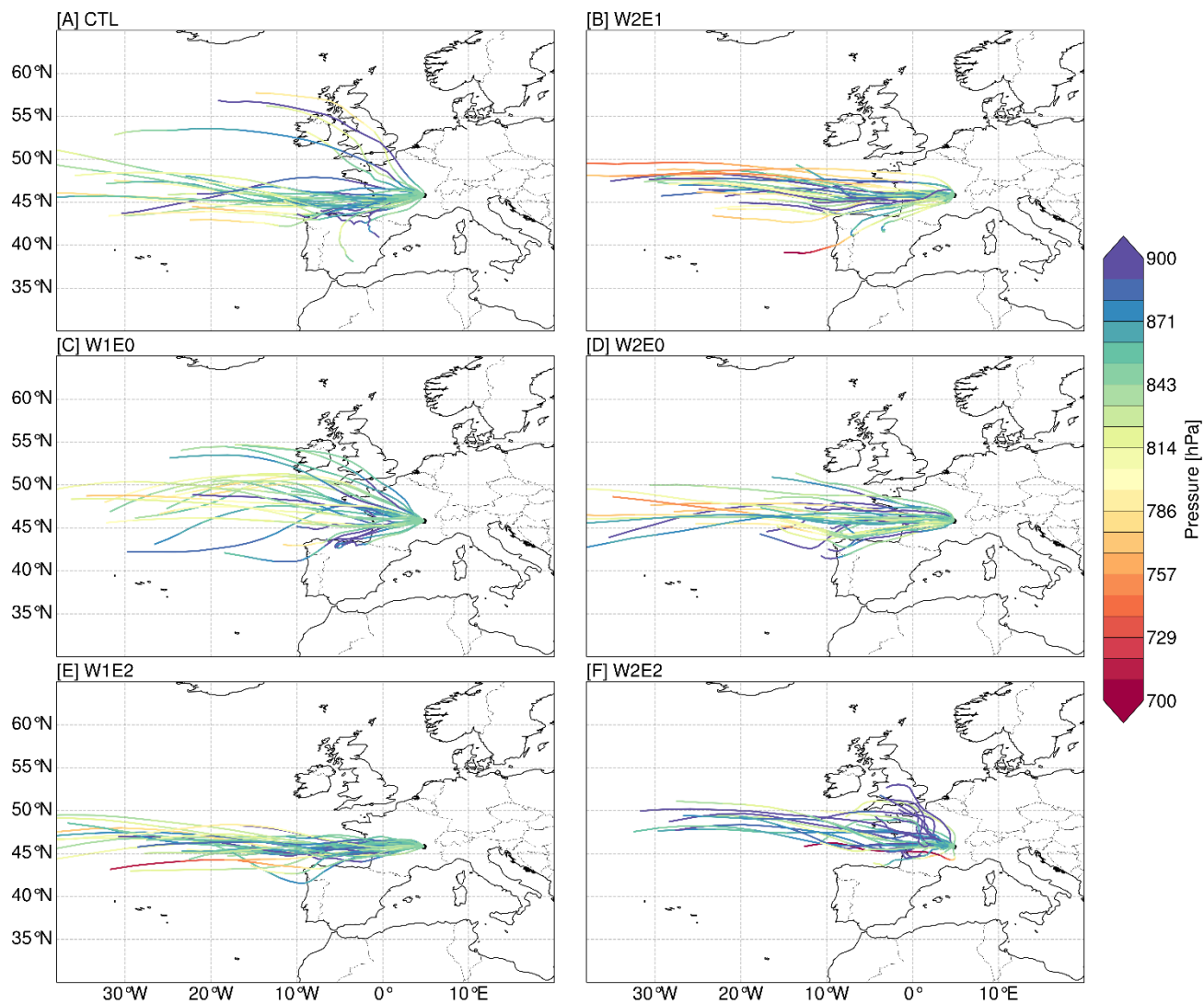
Figure S11: 5 days summer back-trajectories with the receptor location set to the 850 hPa level above Lyon (45.81 °N, 4.82 °E). The colored lines represent the vertical pressure level of the trajectories and were estimated with the 6h model output wind fields using the LAGRANTO tool.

80

Figure S12: 5 days summer back-trajectories with the receptor location set to the 850 hPa level above Munich (48.14 °N, 11.53 °E). The colored lines represent the vertical pressure level of the trajectories and were estimated with the 6h model output wind fields using the LAGRANTO tool.
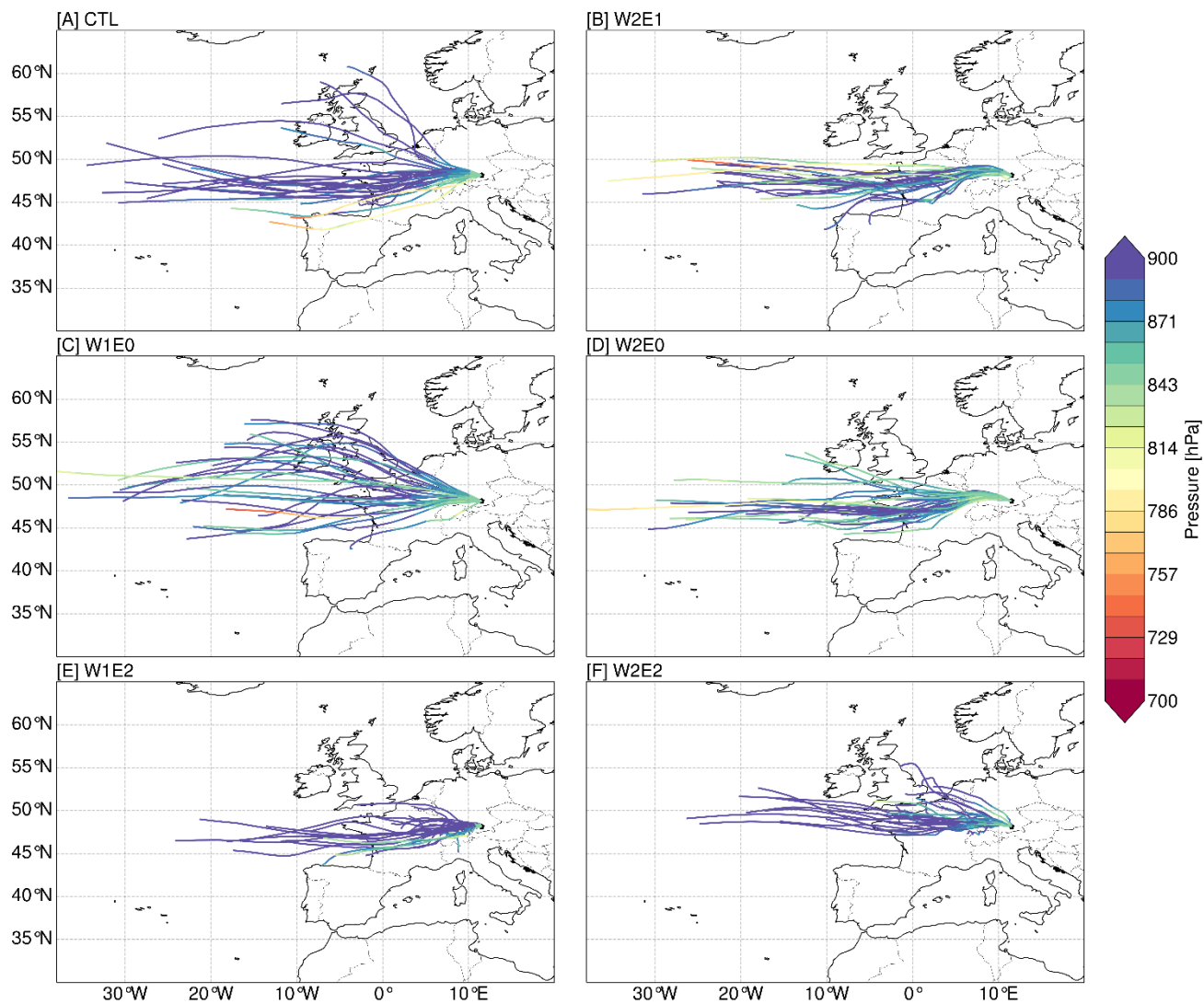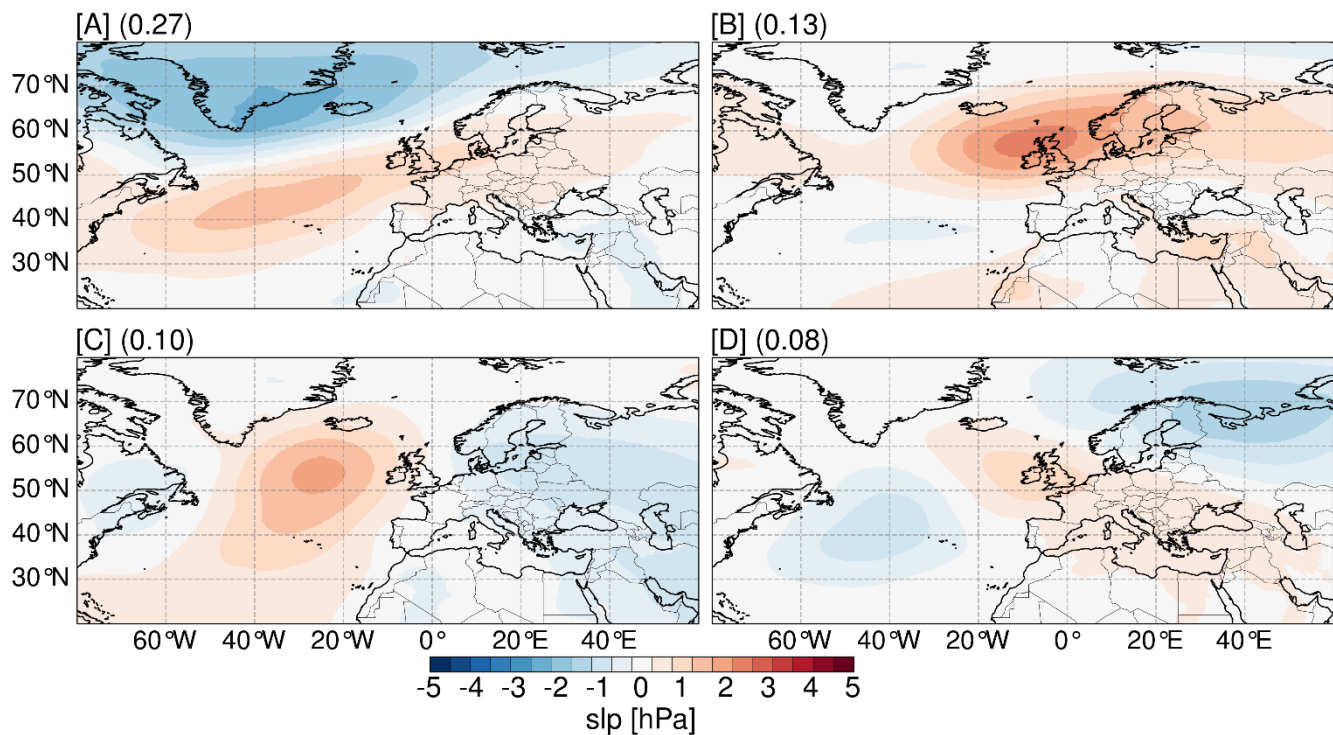
85 **Figure S13: The spatial patterns and explained variance of the first four leading modes of variability extracted from ERA5 summer (JJA) monthly mean sea level pressure (slp) anomalies. The patterns are expressed as the covariance matrix between the time series of the principal components and the EOF of the pressure anomalies.**
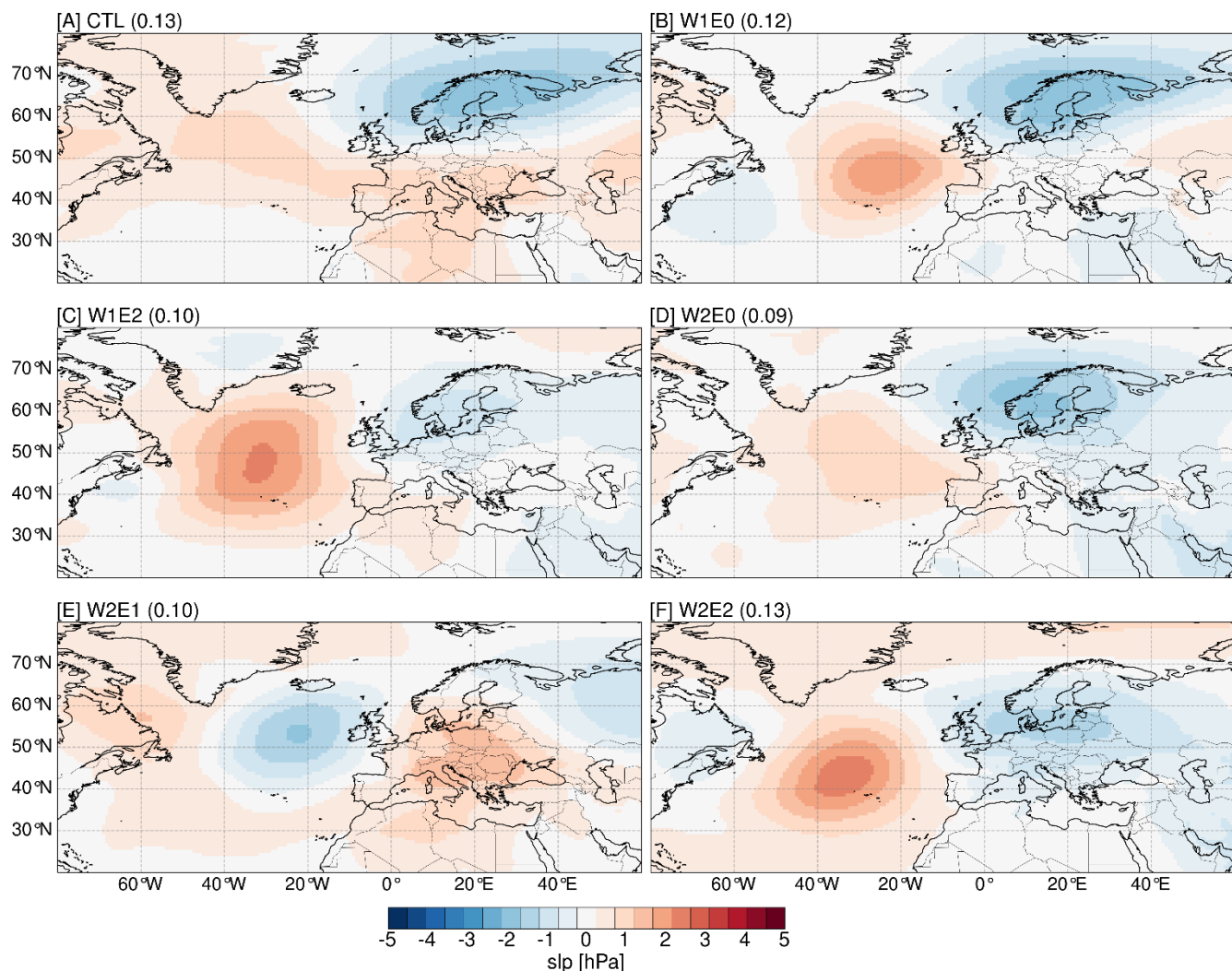
Figure S14: The spatial patterns and explained variance of the EOFs that resemble the third mode variability extracted from ERA5 (Fig. 12) in response to the topographic scenarios. The EOF patterns are estimated from the summer months' means of slp anomalies extracted from the model's output and represent the covariance matrix between the principal component time series and EOFs of the pressure anomalies.

90
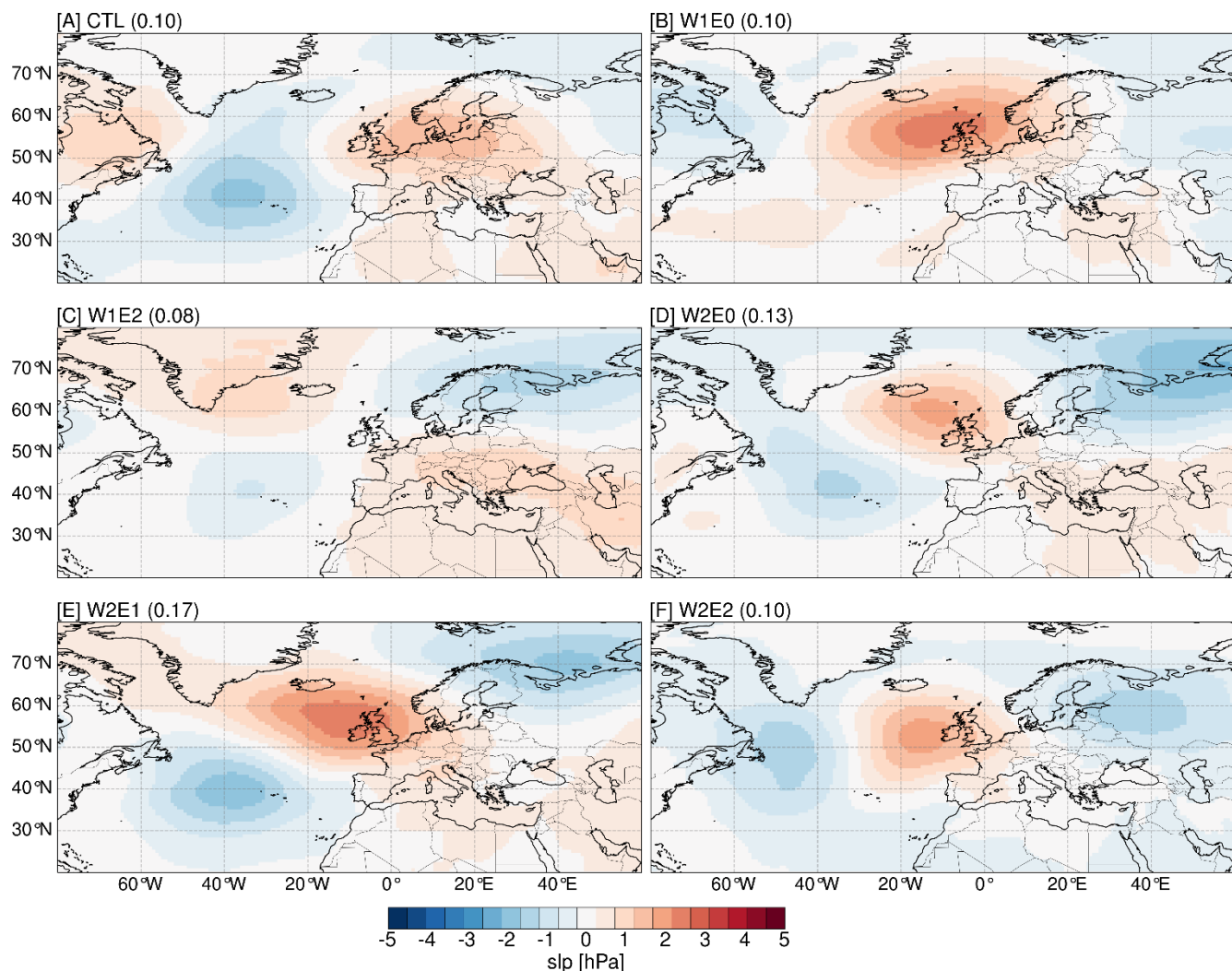
Figure S15: The spatial patterns and explained variance of the EOFs that resemble the fourth mode variability extracted from ERA5 (Fig. 12). The EOF patterns are estimated from the summer months' means of slp anomalies extracted from the model's output and represent the covariance matrix between the principal components time series and EOFs of the pressure anomalies.

95

100